Image-Based Evaluation of Fiber volume fraction in Composite Cross Sections

Sivamayuran Ravichandren

Degree Thesis

Mechanical and sustainable engineering

2025

Degree Thesis

Sivamayuran Ravichandren

Arcada University of Applied Sciences - Mechanical and sustainable Engineering, 2025

Commissioned by:

Erasmus - University of Borås - Arcada University of Applied Sciences

Abstract:

This thesis introduces an innovative, non-destructive way for measuring fiber volume fraction in filament-wound composite tubes using microscopic image analysis and Python-based automation. Recognizing fiber volume fraction's crucial role in defining composite mechanical behavior, the study proposes a digital technique that outperforms traditional destructive testing in terms of precision, repeatability, and efficiency. A carefully structured procedure was carried out on glass fiber composite samples provided by L-Tec Sport, including sample polishing, multi-magnification optical microscopy, and greyscale threshold-based segmentation. Python modules such as OpenCV, NumPy, and Matplotlib were used to classify fibers, matrix, and voids, allowing for pixel-level examination of microstructure with minimal input from users. What highlights this work is the combination of statistical fiber diameter analysis (from over 200 hand-measured fibers, ranged from 29 to 39 pixels) with automated pixel-based fiber volume fraction computation, resulting in findings that nearly match manufacturer data 50-60%. The Python-derived fiber volume fraction values varied from 52% to 55%, while hand computations produced 46-54%. A ±1 pixel inaccuracy in fiber diameter may affect area estimations by up to 77.8% at lower magnifications (magnification of 25X), emphasizing the importance of balancing resolution and accuracy at 100X magnification, the error percentage reduces to less than 5%, indicating the lowest measured error. Edge-based approaches, such as Canny detection, were investigated, but they failed to provide a reliable result. This research is mix of digital image analysis and engineering knowledge establishes a compelling new benchmark for composite material evaluation.

Keywords:

Fiber volume fraction, Composites, Microscopy, Python analysis, Image processing, Thresholding, Glass fiber

Acknowledgements

I would like to convey my heartfelt gratitude to Arcada University of Applied Sciences for giving me the opportunity to conduct this research. I am especially grateful to my supervisor, Rene Herrmann, for his support, insightful feedback, and encouragement, which drove me to obtain greater outcomes and maintain a high standard of work throughout the project.

I am grateful to the University of Borås, especially Professor Mikael Skrifvars, Faranak Bazooyar, Ville Skrifas, and Yones, for their advice and support during my time on campus. Their assistance was critical in the effective execution of this project.

I'd also want to thank L-Tec Sports for donating the composite samples used in this research. A heartfelt thanks to Alexander Clark for his cooperation and kindness for helping this research.

Furthermore, I am grateful to all my lecturers, colleagues, and friends who have encouraged and motivated me throughout this journey. My heartfelt gratitude goes to my family, whose unfailing love, patience, and encouragement have provided a constant source of strength.

Contents

Figures

Tables

1 Introduction

1.1 Background

Composite materials play a crucial role in modern engineering, primarily due to their exceptional strength-to-weight ratios, adaptability, and performance under diverse operating conditions. A key parameter that governs the mechanical and thermal behaviour of these materials is the Fiber volume fraction. The fiber volume fraction directly influences composite properties such as stiffness, tensile strength, and thermal resistance, making its accurate determination vital for both material design and quality control.

In this thesis, a comprehensive analysis of existing literature and experimental studies has been conducted to understand the relationship between fiber volume fraction and composite performance. Research has also compared various methods for fiber volume fraction measurement, ranging from destructive techniques like acid digestion (Asfew, 2024) to non-destructive approaches such as optical image analysis.

Building upon these studies, this work emphasizes cross-sectional image analysis as a non-destructive method, applying microscopy techniques including sample polishing and optical imaging to extract structural data to determine fiber volume fraction. Using Python-based image processing tools, the analysis includes the computation of average fiber radius, as well as quantitative estimates of fiber, matrix, and void volume fractions.

Additionally, a methodical approach is developed to validate and quality-check the extracted data, ensuring the reliability and consistency of results. These studies provide a detailed and reproducible methodology for evaluating fiber volume fraction and related microstructural features in fiber-reinforced composites.

1.2 Relevant Studies

Various methods have been developed over the years to quantify the fiber volume fraction, ranging from traditional destructive techniques to more advanced non-destructive imaging and analysis approaches. These studies reviewed here examine different methods for evaluating fiber volume fraction and related microstructural features, with a focus on microscopy-based

techniques and digital image processing. These studies lay the foundation for the methods applied in the present research.

Measuring the Fiber volume fraction accurately is important for understanding the mechanical properties and consistency of fiber-reinforced composites. Traditional methods like resin burn-off or acid digestion can be destructive and often rely on assumptions about material densities, which can lead to errors. To avoid this**,** the researchers introduced a non-destructive method called optical numeric volume fraction analysis. This approach uses polished cross-sections of the composite, which are then examined under a microscope. High-resolution images are taken, and fiber ends are automatically counted using image analysis software to estimate the fiber volume fraction. This method improves consistency and reduces the influence of human error compared to manual techniques. It also highlights how important good sample preparation and clear imaging are for reliable results. *(Waterbury, 1989)*

The following research uses a Scanning electron microscopy approach to accurately measure the local Fiber volume fraction in non-crimp glass fiber-reinforced composites. Composite cross-sections were prepared using standard metallographic polishing techniques to minimize surface defects and ensure image clarity. High-resolution scanning electron microscopy imaging was performed to capture detailed views of the fiber bundles. The resulting images were then analysed using a combination of manual annotation and automated segmentation in MATLAB. In this work, Otsu's thresholding method was used to convert the grayscale images into binary form, allowing clear distinction between fiber and matrix regions. This process enabled accurate measurement of local fiber volume fraction values across multiple fiber bundles. The study also paid close attention to fiber-rich and resin-rich areas to evaluate how fiber volume fraction varies across different regions within the material. By comparing the fiber packing density at the bundle level with the overall fiber volume fraction, the work aims to assess the reliability and accuracy of scanning electron microscopy image analysis for detailed microstructural evaluation of non-crimp fabric composites. *(Mikkelsen L. P., 2021)*

To examine local variations in fiber volume fraction within non-crimp glass fiber-reinforced polymer composites, the study follows the methodology presented by Mikkelsen and Sørensen, using scanning electron microscopy datasets as both a procedural guide and a benchmark. High-resolution scanning electron microscopy images were taken from polished cross-sections of the composites to clearly reveal the internal structure, including fiber bundles and adjacent resin-rich zones. The images underwent preprocessing steps such as noise reduction and

contrast enhancement, followed by global and adaptive thresholding techniques to distinguish fiber regions from the matrix. Local fiber volume fraction was calculated for each fiber bundle using MATLAB by determining the ratio of segmented fiber area to the total cross-sectional area of each bundle. This approach allows for a more detailed understanding of the composite microstructure and provides higher spatial resolution in fiber volume fraction measurement compared to traditional techniques. *(Mikkelsen, 2023)*

The method is strongly supporting the use of digital image for evaluating fiber volume fraction. Their work compared digital image processing with the traditional resin burn-off method and found that digital image processing offers consistent and reliable results while maintaining the physical integrity of the samples. This is especially useful in studies where repeated imaging or correlations with mechanical testing are required. In the research, similar image processing techniques were applied to both optical and scanning electron microscopy images to assess fiber volume fraction in glass fiber-reinforced composites. The combination of thresholding and segmentation proved effective in separating fiber and matrix regions, particularly when the contrast between them was high. The researcher also demonstrated that accurate fiber volume fraction measurement can be achieved using relatively simple digital tools. Their findings support the use of non-destructive, microscopy-based analysis as a practical and scalable alternative to more invasive or time-consuming methods. This reinforces the potential of digital image processing to serve as a core method in composite material characterization. *(Morales, 2020)*

These studies highlight the progress made in Fiber volume measurement techniques, with an increasing shift from traditional, destructive methods to non-destructive, high-resolution imaging techniques.

1.3 Objectives

1.3.1 General analysis

1. Investigate the Effect of Microscope Magnification on fiber volume fraction Measurement

- By assessing how variations in magnification affect pixel resolution and fiber volume fraction accuracy, the relationship between microscope magnification and fiber volume

fraction calculation accuracy may be evaluated. monitor the frequency of error at various magnifications.

2. Manually Determine Average Fiber Diameter and Its Variation

- By examining at least 3 different images, each containing at least 50 fibers, the fiber diameter may be determined directly. This makes it possible to measure the fiber diameter and its variation.

3. Manually Estimate fiber volume fraction Using Fiber Counting and Image Size

- Fiber volume fraction is quantitatively estimated using the fiber count and picture size. A numerical estimate for fiber volume fraction is created by manually counting fibers and calculating the area they cover compared to the entire image area.

1.3.2 Python analysis

1. Fiber volume fraction Analysis using Python (Pixel values)

- Create a Python-based technique to precisely count the number of pixels in composite material images that correspond to the various material components (fiber, matrix, and voids). The technique makes it possible to precisely calculate and track the fiber volume fraction, which is the proportion of fiber pixels to total pixels.

2. Quality Check fiber volume fraction results Using Canny Edge Detection and Contour Analysis

- Utilize Canny edge detection and contour analysis to extract fiber boundaries as part of an automated process for confirming the fiber volume fraction. To identify fibers, their edges are detected, and their areas are computed using pixels.

By analysing cross-sectional images with Python and comparing the findings to those acquired through manual (hand) computations and density-based calculation, we can validate the image-based method's accuracy. These findings are then compared with results from a density-based computation (From L-Tec sport) to assess the study approach's effectiveness and reliability.

2 Literature Review

This literature review focuses on various methods developed for estimating fiber volume fraction, including microscopic examination, acid digestion, mass and volume measurements, and unit cell modelling. Among these, microscopic examination provides a non-destructive and detailed approach by directly analyzing the composite's microstructure using image processing tools. Recent advancements in digital imaging and computing tools, such as Python-based pixel analysis and thresholding techniques, have improved the accuracy and efficiency of fiber volume fraction computations. This section discusses the ideas, benefits, and limitations of these technologies, with a special emphasis on microscopic examination and automated image processing techniques.

2.1 Fiber volume fraction Calculation Methods

Four different approaches were examined in this section such as, acid digestion, mass and volume measurement, unit cell modelling and microscopic analysis. Analysis of each method was conducted, emphasizing its fundamental ideas, benefits, and drawbacks.

2.1.1 Acid Digestion

One destructive method for figuring out the fiber volume fraction in composite materials is acid digestion. By chemically dissolving the matrix material, acid digestion separates the fibers from the matrix. It is possible to determine the fiber volume fraction by weighing the remaining fibers and using their known density. This test is essential for confirming the predictions of the law of mixtures for composite properties like density or modulus. The equations below (1) (2) describe the methods used to compute the fiber volume fraction. (Asfew, 2024).

$$V_{fiber} = \frac{m_{fiber}}{\rho_{fiber}} \quad (1)$$

$$f = \frac{V_{fiber}}{V_{tot}} \quad (2)$$

Where -

- V_{fiber} - Volume of fiber
- ρ_{fiber} - Density of composite
- m_{fiber} - Weight of the fibers
- V_{tot} - Total Volume of the composite
- f - Fiber volume fraction

2.1.3 Fiber volume fraction via Mass and Volume

Using the masses and densities of the fiber and matrix materials, this approach computes the fiber volume fraction directly. Applying the rule of mixtures to find composite properties requires precise fiber volume fraction determination because Fiber volume fraction is a crucial parameter in the rule of mixtures. This approach (3) is simple and fits in nicely with theoretical frameworks. *(Pan, 1993)*

$$f = \frac{\frac{m_f}{\rho_f}}{\frac{m_f}{\rho_f} + \frac{m_m}{\rho_m}} \tag{3}$$

Where -

- f - Fiber volume fraction
- V_f - Volume of fiber
- m_m - Matrix mass (After digestion)
- ρ_f - Fiber density
- ρ_m - Matrix density
- m_f - Fiber mass

2.1.3 Unit cell modelling

One useful method for calculating the fiber volume percentage in composite materials is unit-cell modelling. With this method, the total fiber content of a composite structure is ascertained by examining its smallest repeating unit. The volume of fiber inside the unit-cell must be

determined to estimate the fiber volume fraction. A 3D model of the unit cell is usually created using CAD software, and the fiber and matrix components are given the required material properties. The accuracy of the fiber volume fraction estimation can be strongly impacted by the unit cell's size and layout. This technique offers important insights for composite design and optimization by enabling a thorough examination of the effects of fiber volume percent on the overall composite parameters, such as stiffness and strength. *(Michael T. Cann, 2008)*

2.1.4 Microscopic analysis

The ratio of fiber area to composite area in optical images is used to calculate the fiber volume percentage. The distribution and orientation of the fibers in the composite can be seen and quantitatively analyzed using optical methods. These techniques analyze the material's cross-sections to assist calculating fiber volume percentage. This check guarantees the validity of the rule of mixes' presumptions regarding appropriate volume fractions and uniform fiber distribution. *(Daniel, 2006)*

$$f = \frac{A_{fiber}}{A_{tot}} * 100 \tag{4}$$

Where -

- f - Fiber volume fraction (%)
- A_{fiber} - Area of fiber
- A_{tot} - Total area of the image

2.1.5 Definition and function of pixels in digital imaging

A pixel is the basic unit of a digital image, representing a single point on a two-dimensional grid. It is the smallest component of an image that may be separately processed or shown. Each pixel has a unique color value and spatial location inside the image matrix. An image is made up of a huge number of pixels, each of which contributes to the overall visual representation. Even though a single pixel is just a plain colored square, when paired with surrounding pixels, it creates visually organized content. The individual pixel blocks are visible in the central

portion of the image, as seen in *Figure 1*, illustrating how each one helps to produce the overall image.

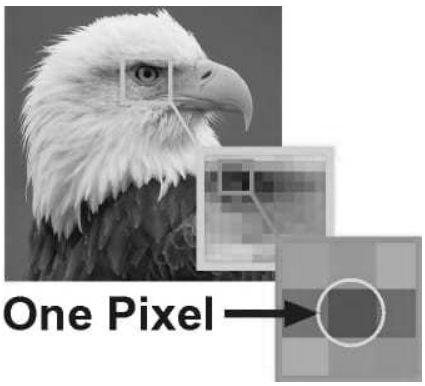

Figure 1. Explanation of 1 pixel, (Simental, 2013)

2.2 Explanation of Fiber volume fraction calculation

With eight pixels arranged horizontally and eight pixels arranged vertically; the image below depicts an 8x8 pixel grid with a total area of 64 pixels.

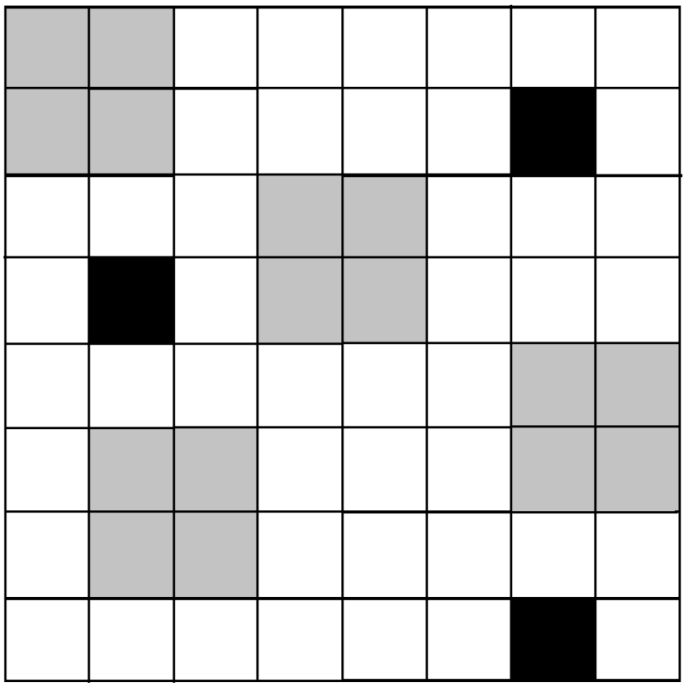

Figure 2. Detailed view of pixels

The grey boxes in the figure are recognised as fiber areas. The black boxes recognised as voids. The whites recognised as matrix. The computation involves figuring out which grey pixels in the image represent the fiber and counting all the pixels in the image. The number of grey

(fiber) pixels is then divided by the total number of pixels to determine the fiber volume fraction.

$$FVF = \frac{Grey\ pixels}{total\ pixels} *100 = \frac{16}{64} * 100 = 25\%$$

In the context of the Python-based calculation, a single-pixel error either exclusion or inclusion can be assessed to determine its impact on the outcome. Assume a total of 64 pixels in the calculation.

Table 1. Impact of Single-Pixel Error on Ratio Accuracy

If one fiber pixel is missed	**If one extra pixel is included**
$FVF = \frac{15}{64} * 100 = 23.4\%$ Then the difference would be 25.0% - 23.4% = 1.6% The error percentage would be = 1.6%	$FVF = \frac{17}{64} *= 26.5\%$ Then the difference would be 26.6% - 25.0% = 1.6% The percentage of error would be = 1,6%

In this situation, a single pixel difference, whether by exclusion or inclusion, introduces an approximate error of 1.6% in the result. This value indicates the estimated margin of error caused by pixel-level imperfections in the Python computation.

2.2.1 Void calculation

In this example, an algorithm determines the void content by recognizing and counting the number of black pixels that represent voids, then dividing that value by the total number of pixels in the image. This method provides a quantitative estimate of the void fraction in the composite cross-section.

$$Voids = \frac{Black\ pixels}{total\ pixels} * 100 = \frac{3}{64} * 100 = 4.7\%$$

Compared to other methods such as acid digestion, resin burn-off and Unit cell modelling, microscopic examination provides a powerful and non-destructive way to determine the fiber volume fraction in composite materials. Digital cross-sectional images are used in this method. The capacity of microscopic analysis to offer comprehensive insights into the orientation and distribution of fibers inside the composite two factors that are essential for forecasting material performance is one of its main advantages.

The investigation of the differences in fiber volume and voids is made possible by microscopy, which permits repeated measurements on the same sample, in contrast to acid digestion, which dissolves the matrix. Although accuracy may be impacted by variables including sample preparation and image quality, when performed correctly, microscopic analysis produces results comparable to those obtained through more conventional techniques. Overall, it serves as a valuable tool for quality assurance and research in composite manufacturing, significantly enhancing our understanding of material behavior.

2.3 Cross section analysis

After the composite tubes were fully manufactured, they were cut at several locations into smaller pieces for the analysis, each approximately 5 mm in length. These small sections were then prepared for polishing and microscopy. The microscopic images taken during analysis represent the specific regions within these polished cross-sections. This visual representation helps provide readers with a clearer understanding of which areas of the composite structure are being examined under the microscope.

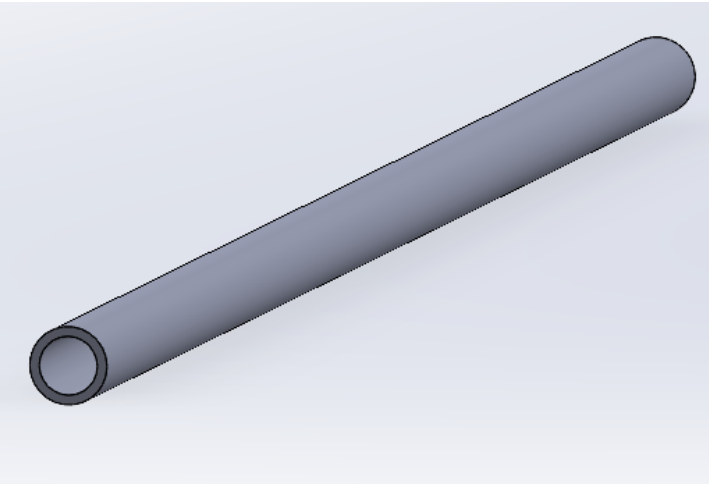

Figure 3. Illustration of a composite tube

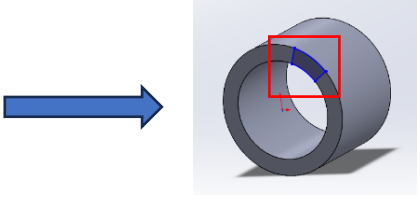

Figure 4. Cut part from tube and intrest of region

To better understand Fiber volume fraction, the study looks at how to utilise Python programs to evaluate cross-sections of composite materials under a microscope. *Figure 6* is a cross-sectional view of a composite material, demonstrating the arrangement and laying of fibers within the structure.

Figure 5. Cross section of a composite tube

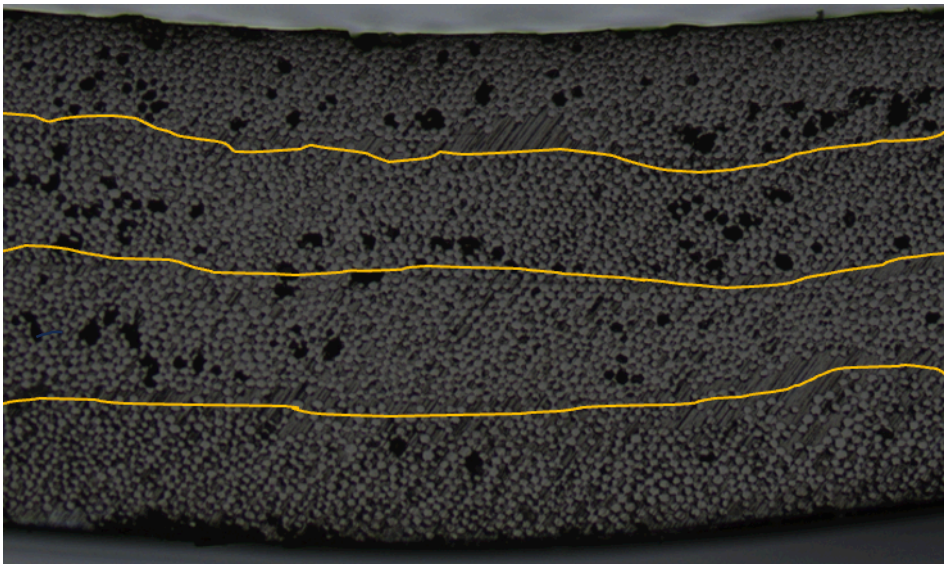

Figure 6. Figure 5 with layer markings

The fiber layers are shown by the yellow lines. *Figures 5* and *6* show the overall properties of the composite material's cross section. *Figures 7* and *8* show a more comprehensive examination of the cross-section, including the surrounding matrix, voids (irregular gaps), and grinder marks.

Figures 7 and *8* illustrate the fibers, matrix, and voids as observed in microscopic images. The fiber dimensions appear to be inconsistent, indicating that size varies. Furthermore, the straight lines shown in the images are identified as grinder marks caused by the polishing process.

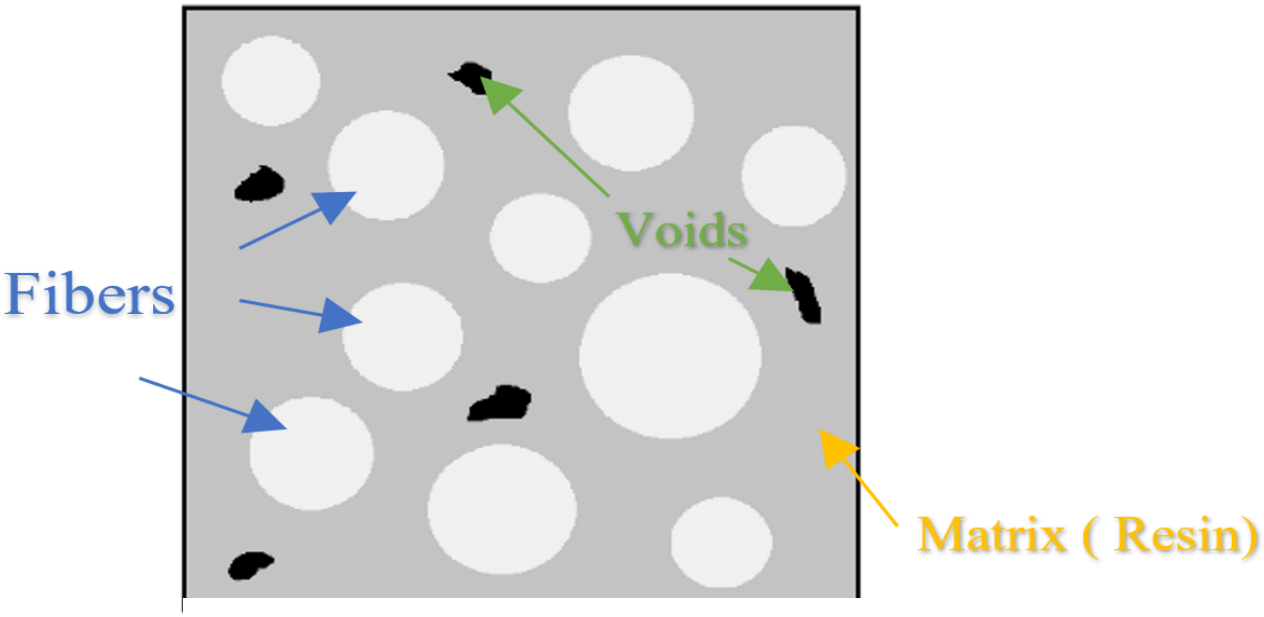

Figure 7. Schematic explanation of cross section

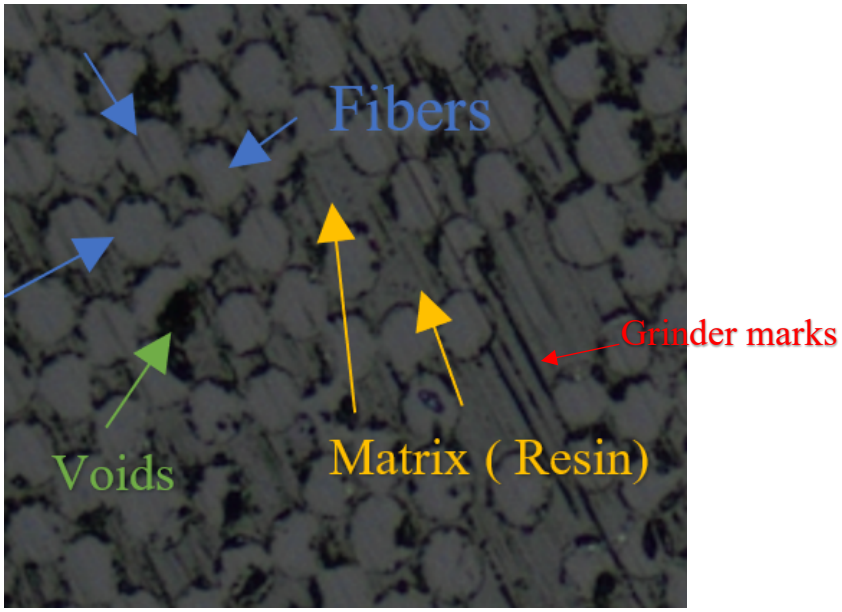

Figure 8. Cross section with markings

2.4 Threshold, Histogram analysis

The numbers on the *Figure 9* vary from 0 to 255. The composite microstructure was segmented into sections using threshold logic developed in Python with the OpenCV. This example uses

three different intensity ranges to categorise by pixel values (The red lines in *Figure 9* are used to visualise the threshold values assigned during image processing). The fiber volume fraction cannot be calculated or visualised without this classification.

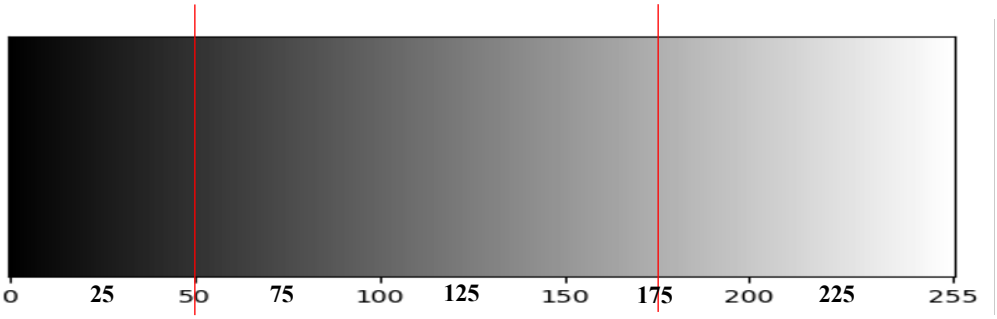

Figure 9. Gray-scale bar (Atul, 2018)

1. **Void Region**

   Void pixels are those whose intensity values fall below the first red threshold line, which in this example is set to 50. To visually identify void regions in the thresholded output image, these pixels are assigned to a greyscale value of zero (black).

2. **Matrix Region**

   In *Figure 9*, pixel intensity levels ranging from 50 to 175 are categorized (The threshold values were found by research on 450+ microscope images. Although no papers were published from that research, it established a threshold value of 175 as best for accurately segmenting the fiber sections) as matrix regions because they fall between the two red threshold lines. In the thresholder output image, these pixels are consistently assigned a gray-scale value of 100 (gray), which allows for clear separation from both void and fiber regions.

3. **Fiber Region**

   Fibers are defined as pixel values that are higher than the upper threshold line, such as 175. These are assigned a value of 255 (white), indicating the fibers in the resulting image.

This segmentation is used to calculate the fiber volume fraction and void content. Based on these parameters, a new image is generated that clearly shows the distribution of voids, matrix, and fibers., which are then displayed along with the histograms. An example is shown below

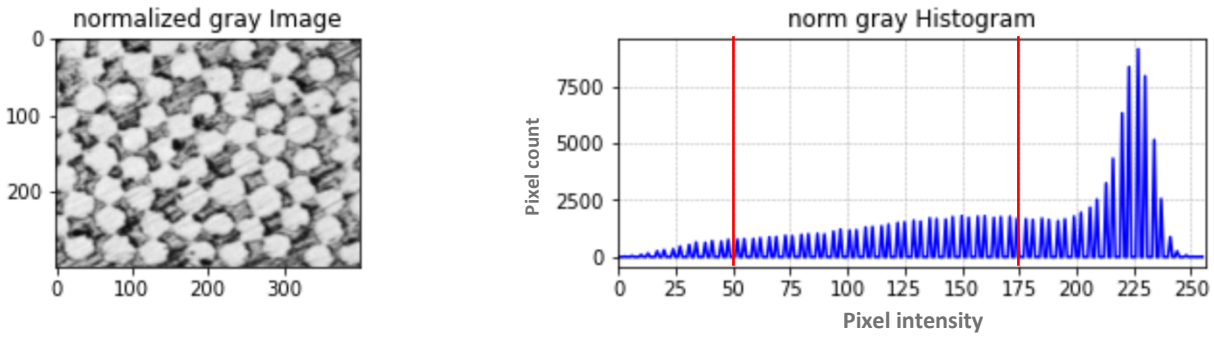

Figure 10. Screenshot of Grayscale image after normalisation and it's histogram

In the histogram, the red lines represent the threshold values set at 50 and 175. Pixel intensity values below 50 are converted to black in the resulting image (*Figure 11*). Pixels with values between 50 and 175 are assigned a gray level of 100 as matrix. Those with values above 175 are converted to white as fiber.

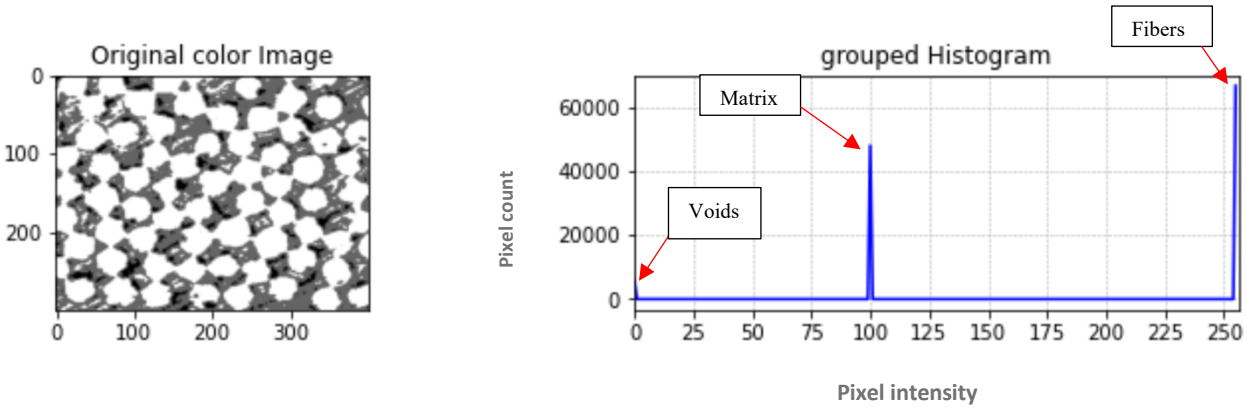

Figure 11. Screenshot of Image generated after thershold seperation and it's histogram

Using these mappings, a new visual representation of the original image is generated. This processed image facilitates further analysis by enabling precise calculations of the Fiber volume fraction and void content. The results of this classification are then presented in the form of histograms, providing a clear statistical overview of the material composition.

3 Experimental procedures

The Experimental procedure for preparing, evaluating, and processing composite material samples to calculate Fiber volume fraction is described in this section. It covers sample preparation, polishing, microscopic imaging and image analysis using Python based workflows.

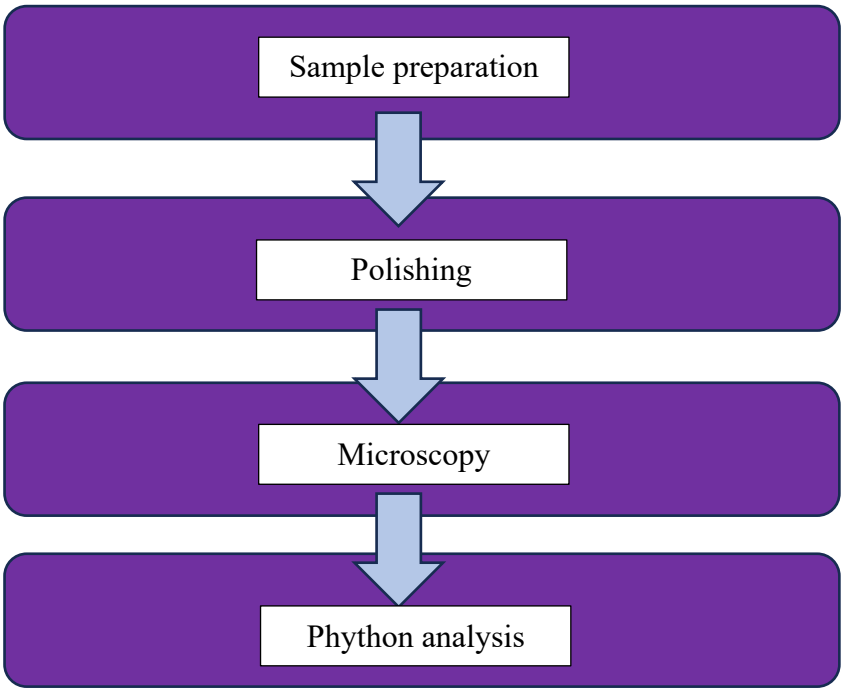

3.1 Sample preparation

Filament winding is a manufacturing technique that involves winding fibers, such carbon or glass, impregnated with resin around a revolving mandrel to produce composite tubes. A mandrel that specifies the final tube size and form is prepared at the start of the procedure. To acquire the required mechanical qualities, resin-saturated filaments are coiled onto the mandrel at precise angles under the direction of automated machinery. A low angle (about 0°) aligns fibers axially for longitudinal strength, while a high angle (about 90°) forms a hoop or circumferential pattern for radial strength. The filament angle is the orientation of the fibers with respect to the tube's axis. The structure is cured to solidify the resin when the winding is finished, and the mandrel is taken out. Across the tube 5 mm size of pieces were cut in different locations. Filament winding took place in the L-Tec Sport company. More than 550 samples have been provided for analysis.

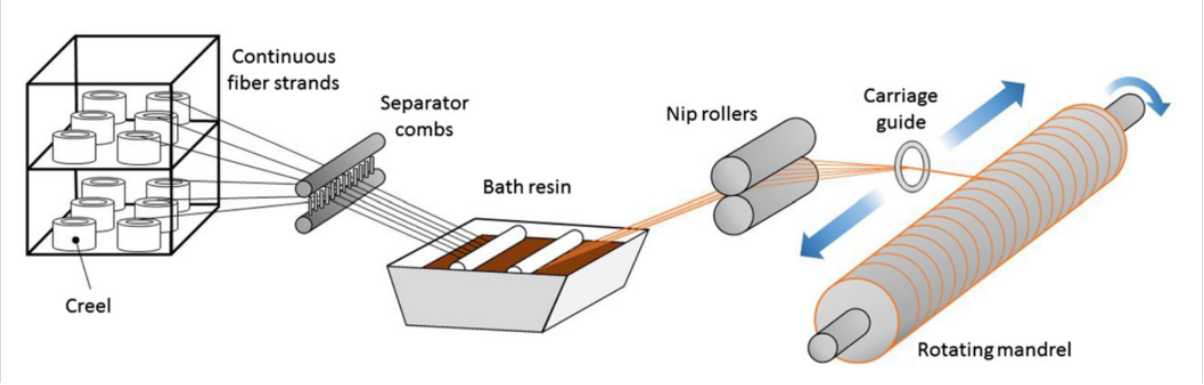

Figure 12. Filament winding process (Addcomposites, 2024)

The methods involved in preparation for polishing are described below. Three to four, 5mm samples were taken per tube. To make identification easier, markers were used to clearly mark each sample as 1, 2, and 3. To further identify the precise side that needs polishing, an arrow sign was added next to the numbers.

Figure 13. Preparation of 27 samples

Figure 14. Samples with markings

3.2 Polishing

The samples were marked, and then the Metaserv 2000 grinding machine was used for grinding them. Throughout the procedure, a modest water speed was chosen. The rotational speed was 250-300 RPM throughout all the procedure. The tube's surface was first polished for one minute using Silicon Carbide 320 grit paper (Polishing paper). After a 90-degree rotation of the samples, Silicon Carbide 600 grit paper (Polishing paper) was applied for an additional minute. After another 90-degree rotation, one minute was spent using Silicon Carbide 1000 grit paper (Polishing paper). Lastly, the water speed was raised, and the samples were rotated 90 degrees once again. The tube's cross-section was then made further polished by using Silicon Carbide 2000 grit paper (Polishing paper) for two minutes. Each sample required five minutes to be processed in total.

Figure 15. Grinder, Metaserv 2000

Figure 16. Polishing papers

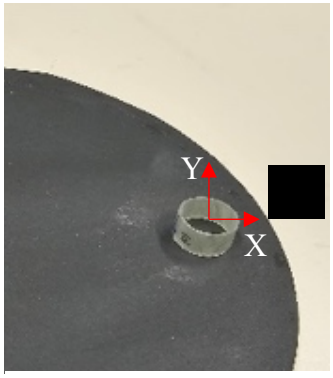

Figure 17. Sample's 1st position while polishing

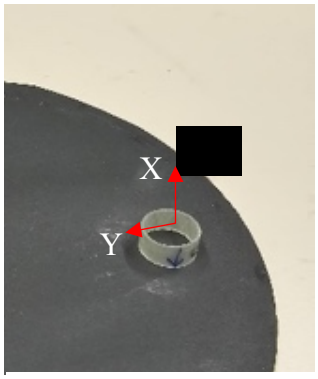

Figure 18. Sample position while polishing with 90-degree rotation

3.3 Microscopy

The samples were captured using the Nikon Eclipse LV100ND microscope. Every sample was carefully positioned in the microscope after it was placed on a glass slide. The samples were carefully moved inside the microscope's range of vision using the joystick. Each sample was image graphed at 25X, 50X, and 100X magnification. The uneven surfaces of several samples produced fuzzy images. A straightforward yet efficient method was utilized to solve this problem. The sample was gently flattened against the lens using forceps and a piece of paper. The image clarity was greatly enhanced by this modification (*Figure 20*).

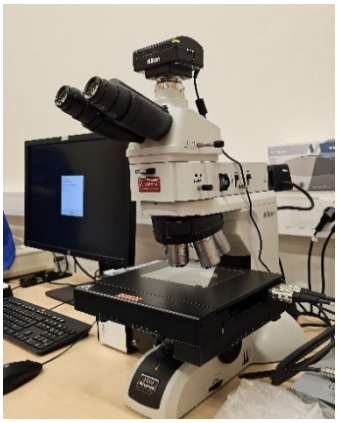

Figure 19. Nikon Eclipse LV100ND

Figure 20. Positioning the uneven flat samples

4 Python Analysis

In this analysis, Python was used to analyze images of the composite tube cross-section captured with a microscope. The image was first cropped to composite region for accurate analysis. Two main image processing methods were applied. The first method calculated the fiber volume fraction by analysing pixel intensity values. The second method used edge detection to identify and map the boundaries of features then check the differences between the images that created by edge detection and the original grayscale image. Together, these techniques provided a clear and reliable understanding of the material's composition and structure.

4.1 Find fiber volume fraction and quality control using pixel values

The algorithm is intended to process a greyscale image, divide it into three unique zones (fiber, matrix, and defect) based on pixel intensity thresholds, and statistically analyse its composition. The OpenCV library was utilized for image processing. Numerical tasks, such as normalisation

and pixel-wise computations, were performed effectively with NumPy, which provides high-performance array operations required for image data processing. Matplotlib was used to visualise images and histograms, providing a clear graphical representation of intensity distributions and segmentation findings throughout the course of the study. The code has been uploaded to GitHub. *(Python-based, 2025)*

4.1.1 Pseudo code

1. **Image loading grayscale conversion**

The method reads an input image with OpenCV and changes it from RGB to greyscale, reducing the data from three channels to one for easier analysis.

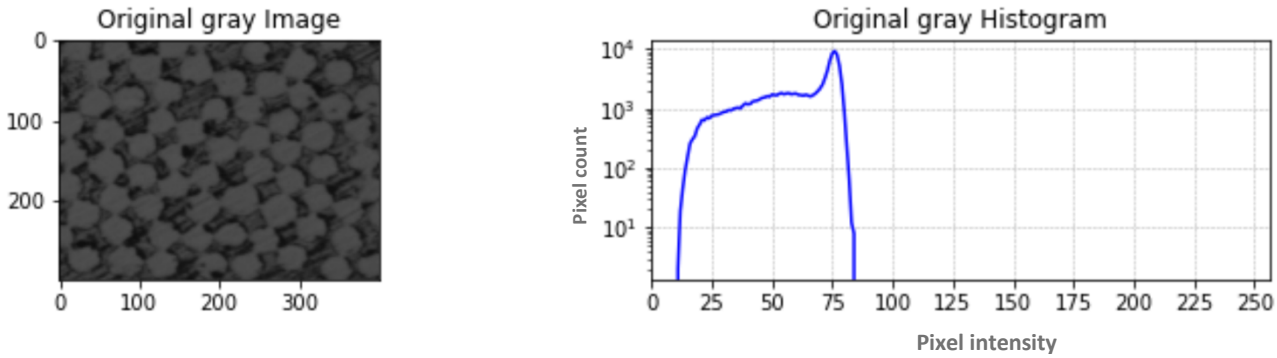

Figure 21. Screenshot of Original gray scale image (100X magnification) and histogram

2. **Normalizing the grayscale image**

The method normalizes the greyscale image by scaling its pixel values from 0 to 255 based on the image's minimum and maximum intensities. This normalization stage increases contrast, making it simpler to differentiate between fibers, matrix, and voids. The normalized image is then utilized for segmentation, which uses intensity thresholds to assign each pixel to one of three material categories. The following equation illustrates the normalization process.

$$I_{normalized\ (x,y)} = \frac{I_{(x,y)} - I_{min}}{I_{max} - I_{Min}} \times 255$$

Where -

- $I_{(x,y)}$ - Original grayscale pixel intensity at position (x, y)
- I_{min} - Minimum pixel value in the image
- I_{max} - Maximum pixel value in the image
- $I_{normalized\ (x,y)}$ - Normalized pixel intensity at position (x, y)

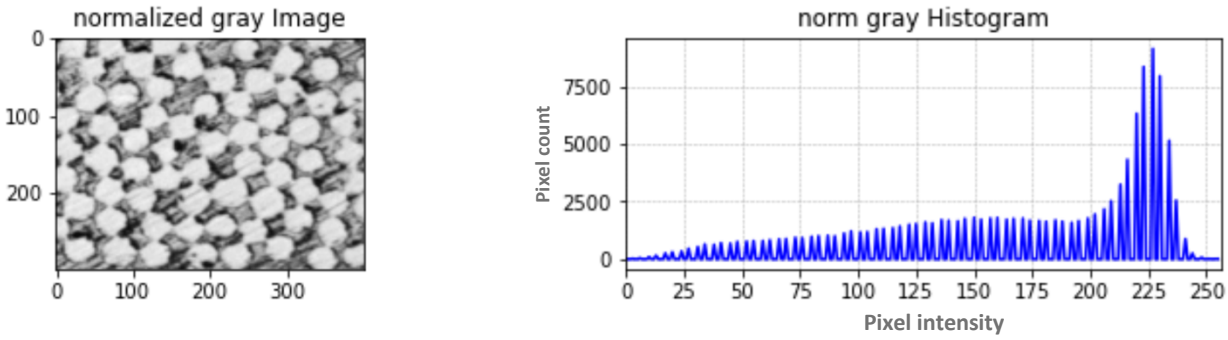

Figure 22. Screenshot of Normalized image (100X magnification) and histogram

3. Segmentation (Fiber, Matrix and Voids)

The normalised greyscale image is divided into three groups using specified intensity thresholds. Each pixel is assigned a new value (255 for fiber, 100 for matrix, 0 for defect) in a new grouped image.

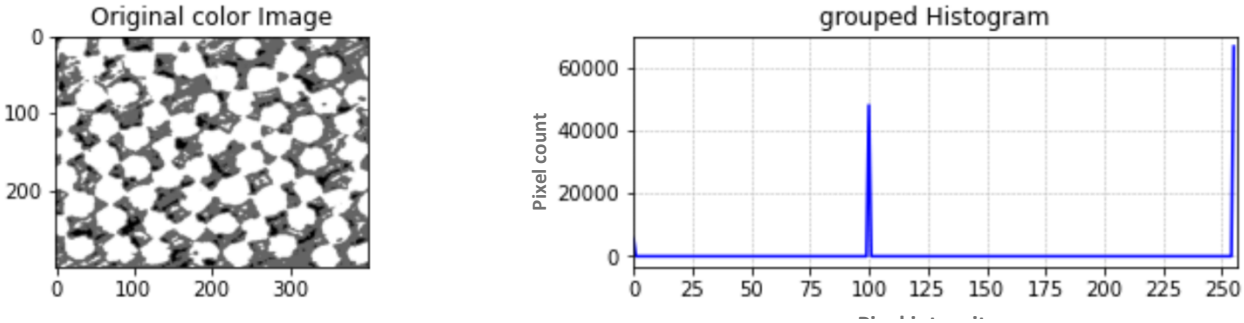

Figure 23. Screenshot of Segmented image (100X magnification) and Histogram

4. Analysis

The code analyses an image by calculating various key statistics. First, it calculates the total number of pixels and examines the image's dimensions. It also determines the lowest and maximum pixel values in the original image. Then it counts how many pixels are in each segmented class fiber, matrix, and voids. It then estimates the percentage of fiber and defect pixels relative to the total, giving a precise assessment of the image's composition.

```
Minimum pixel value - 11
Maximum Pixel value -  84
Vertical Length: 300
Horizontal length: 400
Total area: 120000
Fiber count: 66506
Matrix pixel: 47889
Defect pixel: 5605
Count of fiber+ matrix+ defect : 120000
Fiber volume fraction : 55.42166666666667%
Void fraction: 4.670833333333333%
Normalized grayscale value in the original image : 55
The classification of the pixel in resultend image: 100
```

Figure 24. Screenshot of Computation results by python code

5. **Pixel-by-Pixel Comparison and Validation (Quality Check)**

The original image is compared to its thresholded version by checking each pixel location. To visualize the accuracy of the thresholding, a third image is generated: pixels where the original and thresholded images match are shown in white (255), while mismatches appear in black (0).

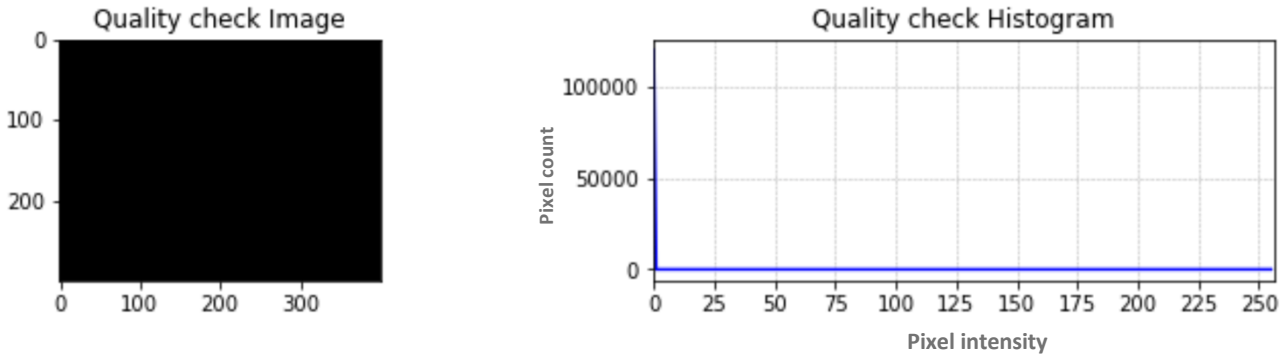

Figure 25. Screenshot of Quality check image (100X magnification) and its histogram

4.2 Edge Detection and Contour Mapping Using Canny Algorithm

This part of code detects and visualises the boundaries of features within a greyscale image using edge detection and contour mapping methods. The Canny edge detection algorithm *(Canny, 1986)* is used to detect strong intensity gradients that frequently correlate to the edges or limits of objects. These discovered edges are then utilised to extract contours, which are created and filled in on a blank image for visualisation. The code compares two images by inspecting each pixel to see whether it has changed. It then generates a new image that emphasises just the pixels that differ. Following that, it counts the number of pixels that have changed and calculates the variance. Finally, it calculates the ratio of altered pixels to total pixels to determine how much the image has changed overall. OpenCV and Matplotlib were used to implement image analysis. The code has been uploaded to GitHub. *(Shape-Detection, 2025)*

4.2.1 Pseudo code

1. **Image Loading and Grayscale Conversion**

   The input RGB image is read using OpenCV and transformed to greyscale format, reducing processing complexity by working with a single intensity channel.

2. **Initialization of Cleared Images**

   Setting all pixel values to 255 creates two blank white images. These are used as panels to see contour findings and as a quality control image.

3. **Canny Edge Detection**

   The greyscale image is processed through the Canny edge detector with threshold values of 100 and 200 (Selected from pixel values of fiber and matrix). This recognises locations in the image with large spatial intensity gradients, indicating edges.

4. **Contour Extraction and Drawing**

   OpenCV's find Contours algorithm extracts contours from an edge-detected image. Each contour is then rendered as a filled shape on a blank image to highlight the structural elements that have been found.

5. **Visualization**

Three images are displayed side-by-side as output. Below the image, the total number of pixels, the number of pixels that changed between the images, and the ratio of changed pixels will be displayed.

- The original grayscale image
- The modified image with filled contours
- The Compared and Quality control image

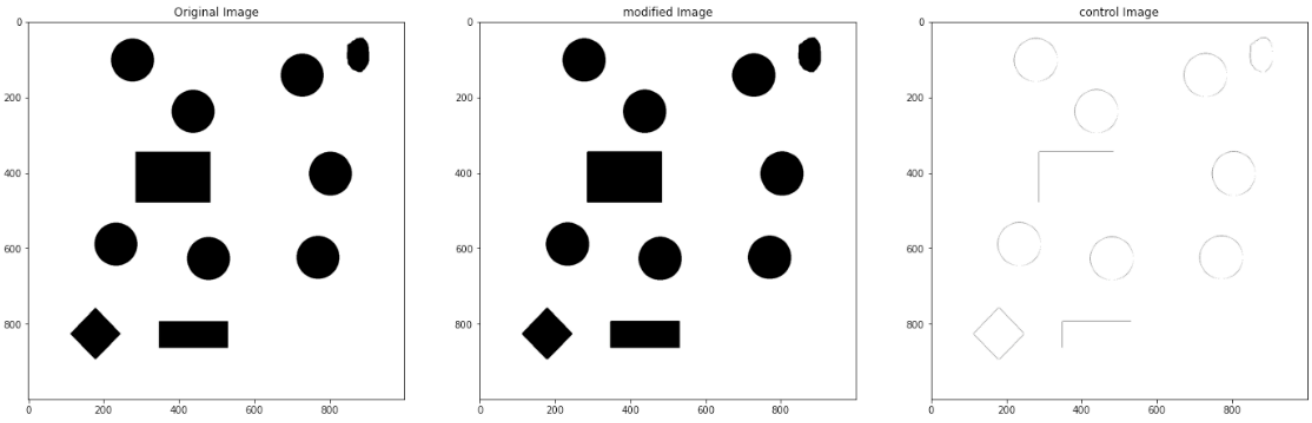

Figure 26. Screenshot of sample images of shape detection

```
Number of pixels that have been changed: 2263
Total number of pixels: 1000000
Ratio of changed pixels to the total number of pixels: 0.002263
```

Figure 27. Screenshot of the resulted Calculation from python

5 Results

5.1 Diameter analysis with different magnification

All samples were analyzed using pixel-based measurements. GIMP software was used to measure the fiber diameters from the images. Images were expanded, and measurements were taken on over 100 fibers for each image. The findings were documented, and the data is shown in Table 2. At 25X magnification, fiber sizes ranged from 4 to 8 pixels. At 50X magnification, the diameters ranged from 10 to 16 pixels, whereas at 100X magnification, they were 20 to 46 pixels.

Table 2. Magnification vs Diameter range

Magnification	25X	50X	100X
Diameter of Fiber (Pixels)	4-8	10-16	20-46

Figure 28. Cross section view of glass fiber sample at Magnification 25X

Figure 29. Cross section view of glass fiber sample at Magnification 50X

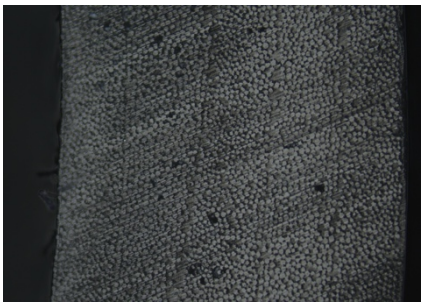

Figure 30. Cross section view of glass fiber sample at Magnification 100X

5.2 Analysis of Area Measurement Error Due to Single-Pixel Diameter Variations

This graph highlights the sensitivity of fiber area calculations to tiny deviations in observed diameter. It focusses on the inaccuracy caused when the diameter is mismeasured by only ±1 unit often equivalent to a single pixel in digital imaging. The data is categorized by magnification levels (25X, 50X, and 100X) to show how measurement error varies between scales.

The fiber area is computed using the standard formula for the area of a circle ($A = \pi r^2$). A tiny change in diameter causes a nonlinear change in area. As seen in the graph, even a 1-pixel error in diameter measurement can result in a considerable percentage error in computed area, particularly at lower diameters (for example, a 1-pixel underestimating of diameter 4 as 3 at 25X magnification results in a 77.78% error in area). This imbalance is especially noticeable at smaller fiber diameters and lower magnifications, where each pixel makes up a greater proportion of the entire measurement.

As magnification increases, the relative inaccuracy reduces because the size of a single pixel becomes a smaller part of the overall diameter. At 100X magnification, a ±1 pixel discrepancy in diameters (46-47) leads in an area inaccuracy of about 4-5%. The goal of this analysis is to highlight the significance of exact diameter measurements in fiber analysis and to calculate the potential error margin caused by modest measurement mistakes. This helps to validate the accuracy of fiber area calculations and emphasizes the importance of high-resolution imaging and thorough manual measurement techniques.

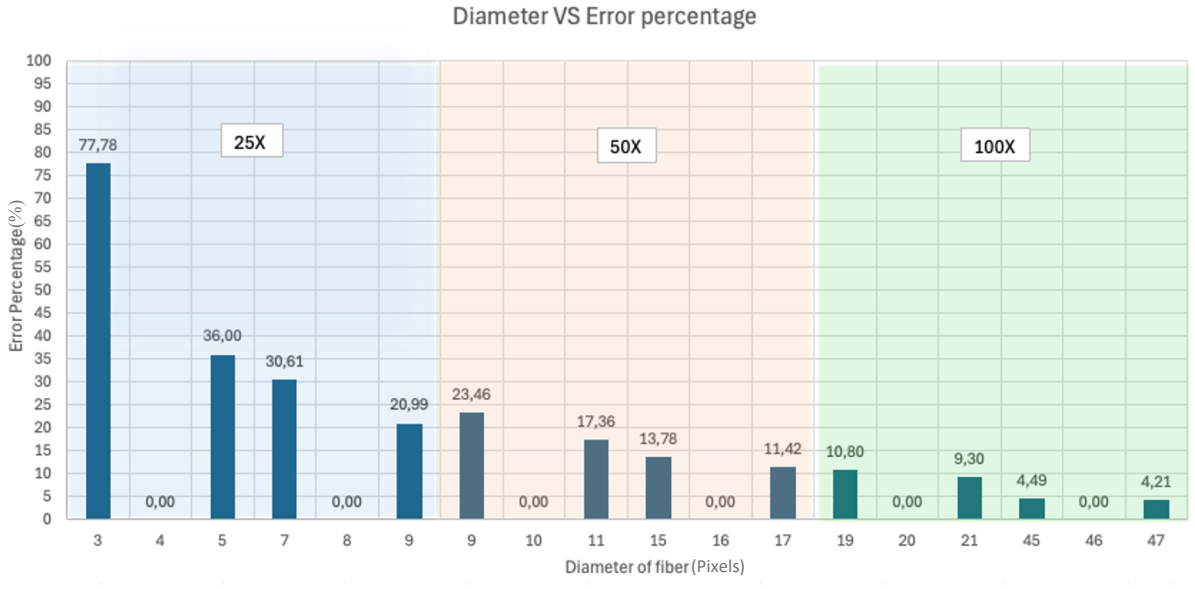

Figure 31. Diameter VS Error percentage graph

For the following analysis, four microscopic images were chosen, each at a magnification of 100X. These images were chosen to provide a representative sample of the fiber structure under consistent imaging settings. The selected images below have a resolution of 400×300 pixels, allowing for reliable measurement and evaluation of fiber sizes.

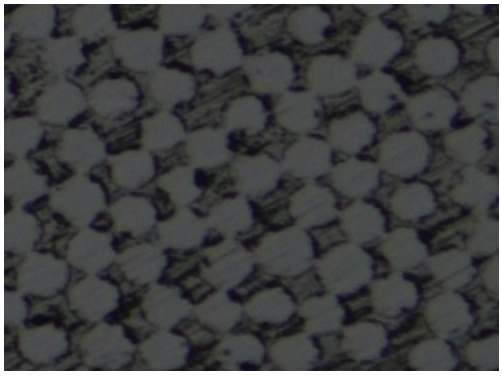

Figure 32. Sample image 1

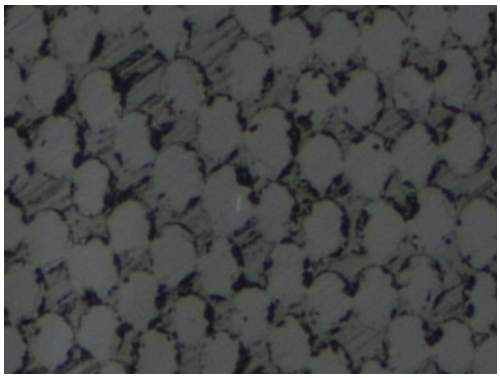

Figure 33. Sample image 2

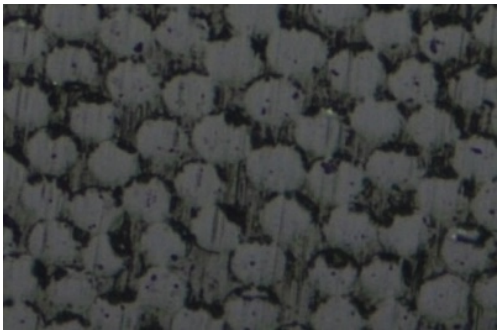

Figure 34. Sample image 3

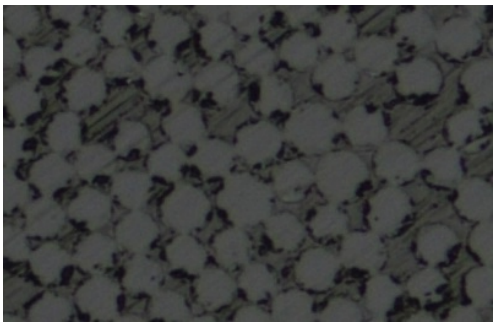

Figure 35. Sample image 4

5.3 Manually Determine fiber volume fraction

The sample images were examined to manually calculate the fiber volume fraction of the composite samples. Every fiber that could be seen in each image was measured and counted. Full and half-visible fibers were both included, the average diameter has been provided to the half-visible fibers. The diameters of the fibers were measured in pixels, and the fiber volume fraction was calculated using the geometric characteristics obtained from the measurements.

5.3.1 Statistical Analysis of Fiber Diameters

The fiber sizes for every image were statistically evaluated. To comprehend the range of fiber sizes, the mean (average), standard deviation (Stdev), and diameter range were computed.

Table 3. Fiber Count and Diameter Statistics

Sample images	Fiber count (Full+Half) (Pixels)	Average Diameter (Pixels)	Standard Deviation (Pixels)	Minimum Diameter (Pixels)	Maximum Diameter (Pixels)	Range (Pixels)
1	63+9	32.64	3.36	22.63	41.53	18.9
2	45+20	38.69	2.58	33.63	45.8	12.17
3	51+19	36.04	3.13	29.00	41.8	12.8
4	69+24	29.29	4.08	20.27	39.27	19.00

5.3.2 Graphical Representation of Fiber Diameter Distributions

Figure 38 illustrates a histogram of fiber diameter distributions from four separate samples. This visual representation provides a detailed visualization of the frequency of fiber diameters within the observed range, increasing the understanding of the data beyond only numerical summaries. Each curve in the plot represents a different sample: Sample 1 (light blue), Sample 2 (dark green), Sample 3 (orange), and Sample 4 (dark blue). The x-axis represents fiber diameter, and the y-axis shows the number of fibers in each diameter range. The graphs indicate that the distributions of fiber sizes fluctuate between samples, with changes in both the trend and spread.

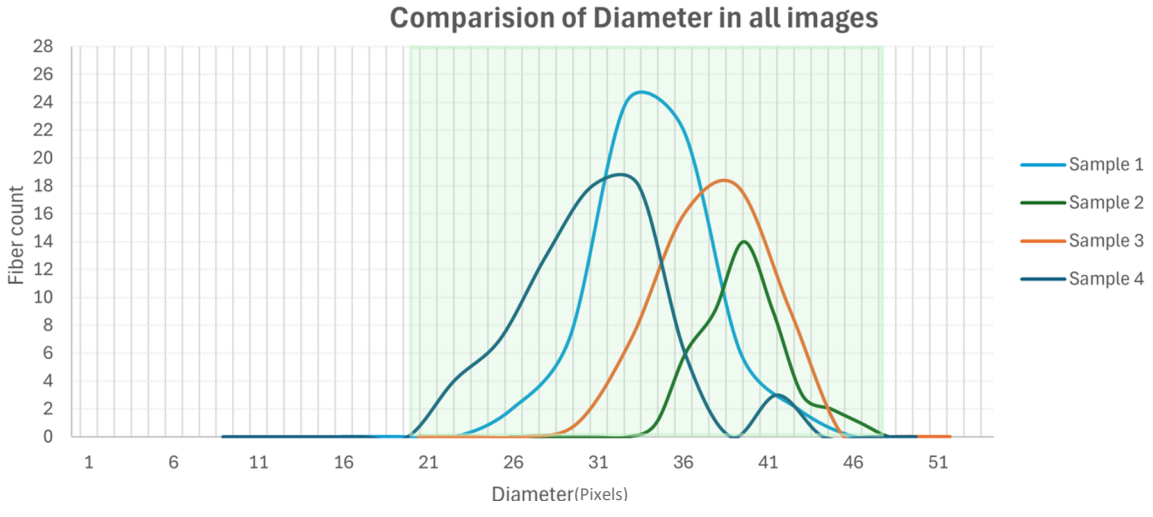

Figure 36. Diameter Comparison of all samples (100X magnification)

5.3.3 Fiber Count and measurement Summary

The summary of manually determined fiber characteristics for four sample images is shown in Table 6. The average diameter of the visible fibers in each image was calculated by counting all of them. The fiber volume fraction which indicates the percentage of the image area occupied by fibers, was computed using these values. Based on mathematical assumptions, the results have a statistical uncertainty of about ±2%. A measured value of 52% would be represented as 52% ± 1% in fiber volume fraction, which corresponds to an absolute uncertainty of 1%. Void area within the images couldn't be measured manually, so they have been excluded from the calculations. The fiber volume fraction values presented here may therefore minimise the overall void fraction in the composite structure because they only take into consideration the observable fiber portion. The results show a reasonably uniform fiber distribution throughout the sampled locations despite of this restriction.

Table 4. Diameter and Fiber volume fraction analysis

Sample images	Fiber count in pixels (Full + half)	Average Diameter (Pixels)	Cross-sectional area of the fibers (Pixels)	Fiber volume fraction + Uncertainty
1	63+9	32.64	57020	48% ± 1%
2	45+20	38.69	64903	54% ± 1%
3	51+19	36.04	62108	51% ± 1%
4	69+24	29.29	55480	46% ± 1%

There was some variation in the distribution of fibers among the images, as seen by the fiber count, which ranged from 45 to 69. Image 2 has the highest fiber volume fraction (54%), even though it has the fewest fibers. This suggests that a bigger volume percentage can be occupied by fewer but larger fibers. On the other hand, Image 4 has the lowest fiber volume fraction (46%) due to its smallest average diameter (29.29 pixels) and maximum fiber count (69).

These findings highlight how fiber diameter has a significant impact on the final fiber volume fraction. Although volume occupancy is influenced by the number of fibers, the overall fiber volume fraction is mostly determined by the cross-sectional area, which is proportional to the square of the diameter. The relationship is consistent with the theoretical prediction that fiber volume fraction rises as fiber size and quantity.

5.4 Python Analysis

5.4.1 Fiber volume fraction and Quality control using pixel values

This section presents the findings of categorising and processing greyscale images for fiber volume analysis. The previously mentioned threshold-based classification technique was used on four 400 × 300 pixel pictures of composite samples. The goal was to calculate the area fractions of the fibers and voids. The following chart displays the findings of the Python analysis.

Table 5. Python analysis results

Sample images	Total pixels	Fiber pixels	Matrix pixels	Defect pixels	Fiber volume fraction	Void fraction
1	120000	66506	47889	5605	55%	4.7%
2	120000	62704	50639	6657	52%	5.6%
3	120000	66067	36226	17707	55%	14.0%
4	120000	63123	49643	7234	53%	6.0%

5.4.2 Canny edge detection

Although Canny edge detection detected certain boundaries, it struggled to reliably capture and fill objects on a consistent basis. The edges discovered by Canny, while existent, were frequently insufficient to establish a complete, continuous boundary. As a result, the image's shapes were not properly filled, producing partial and untrustworthy findings.

With continuous research and acceptance of newer methods, it is expected that more precise and dependable results in composite material analysis can be accomplished. This work is a starting point, it has the potential to improve greatly. The images shown below demonstrate boundary detection and shape filling results comparing with the original sample images.

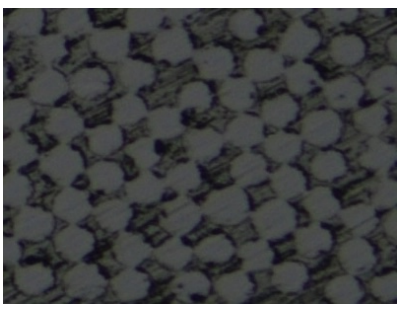

Figure 37. Sample image 1

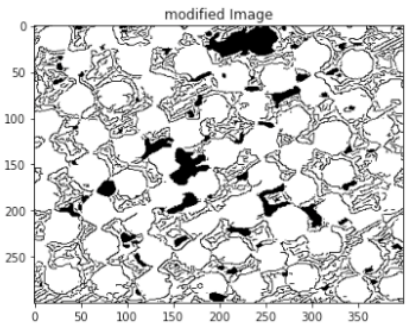

Figure 38. Canny edge detection for Image 1

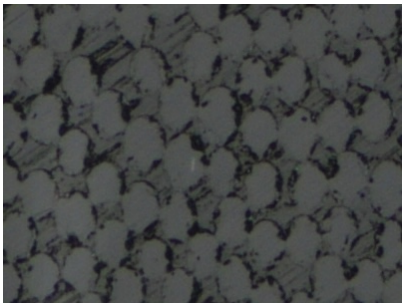

Figure 39. Sample image 2

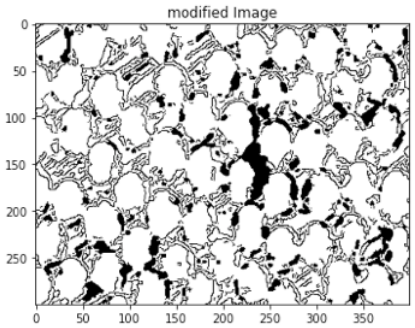

Figure 40. Canny edge detection for Image 2

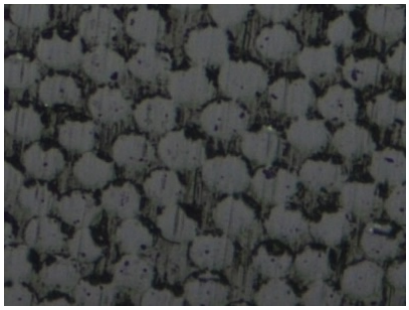

Figure 41. Sample image 3

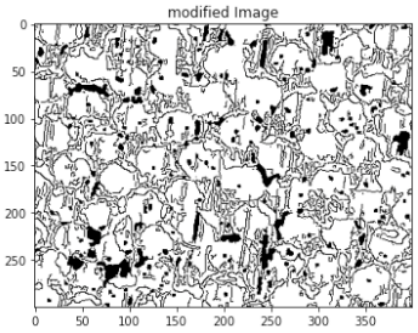

Figure 42. Canny edge detection for Image 3

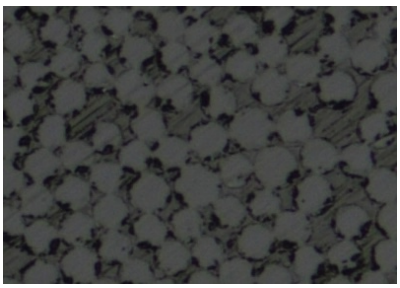

Figure 43. Sample image 4

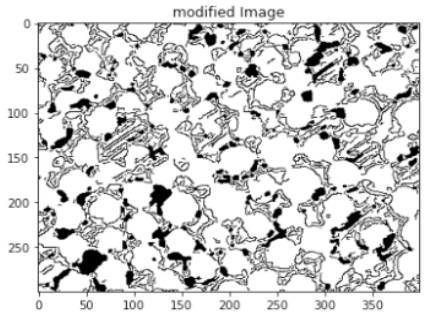

Figure 44. Canny edge detection for Image 4

5.5 Comparison of python analysis and manual calculations

Table 6 compares the fiber volume fraction values produced using three distinct methods: Python-based image analysis, manual hand calculations, and the manufacturer's density-based technique. The results are generally consistent across all approaches, with minor differences due to image resolution, operator estimation error, and potential variances in density assumptions. The Python-derived findings somewhat exaggerated fiber volume fraction in some circumstances when compared to manual calculations, which is most likely owing to the algorithm's sensitivity in pixel intensity thresholding. Nonetheless, all findings are within the manufacturer's specified range 50-60%, demonstrating the validity of both automatic and human procedures.

Table 6. Comparison of the results for fiber volume fraction

Image numbers	Python results (Fiber volume fraction)	Hand calculation result (Fiber volume fraction)	Density based calculation (Fiber volume fraction)
1	55%	48% ± 1%	50-60%
2	52%	54% ± 1%	50-60%
3	55%	51% ± 1%	50-60%
4	52%	46% ± 1%	50-60%

5.6 Comparison of python vs hand calculation by fiber area

Further to test the accuracy of the Python-based fiber volume analysis, a total fiber area (in pixels) comparison was performed for each image using the automated technique and manual hand estimates, as shown in Table 7. The differences range between - 2,199 pixels (Sample image 2) to +9,486 pixels (Sample image 1). This variance could be due to changes thresholding values and rounding in hand calculation. The ±2% uncertainty range in hand calculations accounts for human error in fiber diameter estimation and counting. Despite these differences, the observed deviations are within a respectable range, verifying the Python-based approach's consistency and emphasising the necessity of accurate calibration and threshold setting in automated image processing.

Table 7. Pixel wise comparison graph of fibers

Sample image	Python Calculation (Pixels)	Hand Calculation (Pixels)	Difference in pixels (Python-hand calculation)
1	66506	57020 ±2%	9486
2	62704	64903 ±2%	-2199
3	66067	62108 ±2%	3959
4	63123	55480 ±2%	7643

6 Discussion

The comparison of python-based image analysis to hand calculations and density-based values (*Table 6*) demonstrates a strong agreement, confirming the accuracy of automated fiber volume

fraction estimation and quality check. In general, the image processing using OpenCV produced slightly higher fiber volume fraction values, owing to its sensitivity to pixel intensity thresholds and probable overestimation in detecting bright fiber sections. However, the differences were within ±2%, which is suitable for most technical applications. The manual method, although more time-consuming, produced consistent findings with well-defined uncertainty margins. This validation verifies the image processing using OpenCV approach's accuracy when images are of high quality and thresholding is properly calibrated.

The Canny edge detection technique failed to produce good results. Despite trying with a variety of threshold levels, the algorithm repeatedly failed to detect distinct fiber boundaries. The edge maps generated were either overly simple or overloaded with noise, indicating a poor response to image properties. As a result, Canny-based segmentation was declared ineffective for this dataset. Further exploration and development of this approach could lead to better outcomes. This Python code can be considering an early attempt in the larger context of composite material analysis, and with more adjustments, it may produce superior results.

The observed differences in fiber area (up to ±9.486 pixels) between manual and Python calculations highlights the importance of careful parameter optimisation in digital workflows. In python calculations, void content estimations added in the analysis by finding internal faults.

Combining Python-based image processing with manual verification and manufacturer benchmarks resulted in a comprehensive, multi-level validation methodology. The findings support the use of image-based digital analysis as a dependable, scalable, and non-destructive method for assessing microstructural properties in composite materials.

In this work, the fiber volume fraction was calculated using a colour ratio technique, with the colour fraction serving as a representation of fiber content. While this method is simple and successful under consistent imaging settings. An alternate way would be to use feature recognition to identify specific fibers, such as objects, circles, ellipses, or contours, and calculate their area. This geometry-based method enables direct quantification of fiber presence based on shape and size, providing a more structural and understandable measurement of fiber volume fraction. This could be an effective way one could be able to try in future studies.

7 Conclusion

This thesis effectively presents a reliable and non-destructive approach for estimating fiber volume fraction in composite tubes via microscopy and Python-based image processing. The automatic analysis produced results that matched manual calculations and manufacturers' data, demonstrating it's accuracy and efficiency. Key results include:

- Manual computations confirmed the correctness of the automated approach and demonstrated the effect of fiber diameter on fiber volume fraction. Manual analysis of over 200 fibers across numerous images enabled accurate fiber diameter measurement and statistical analysis, including average diameter, standard deviation, and range. The measurements confirmed manual estimation of fiber volume fraction using fiber count and area-based methods, with findings within a ±2% uncertainty limit.
- Python analysis produced fiber volume fraction values in the appropriate 50-60% range for all samples. The program accurately targeted between fiber, matrix, and void regions, yielding reliable fiber volume fraction results that were consistent with both manual calculations and manufacturer-supplied density-based values 50-60%. Minor inconsistencies were identified and assigned to threshold sensitivity, void inclusion, and image quality variation.

This study supports digital image analysis as a scalable, repeatable, and accurate alternative to traditional fiber volume fraction measuring procedures in composite manufacturing. Future research could increase automation by including machine learning for feature recognition and adaptive thresholding.

References

Pan, N. (1993). *Theoritical detemination of the optimal fiber volume fraction and fiber-matrix property compatibility of short fiber composites.* Plo.

Michael T. Cann, D. O. (2008). *Characterization of Fiber Volume Fraction Gradients in Composite Laminates.* Journal of Compostie Materials.

Daniel, I. M. (2006). *Engineering Mechanics of Composite Materials.* Oxford University Press.

Waterbury, M. &. (1989). *Determination of fiber volume fractions by optical numeric volume fraction analysis. Journal of Reinforced Plastics and Composites.* Retrieved from https://www.researchgate.net/publication/241439502_Determination_of_Fiber_Volume_Fractions_by_Optical_Numeric_Volume_Fraction_Analysis

Mikkelsen. (2023, June). Retrieved from https://www.sciencedirect.com/science/article/pii/S2352340923001762

Morales, C. N. (2020, November). Retrieved from https://www.sciencedirect.com/science/article/pii/S1359836820333564

Simental, C. (2013, March 28). *Ripe media*. Retrieved from https://www.ripemedia.com/why-i-love-pixels-and-so-can-you/

Atul, K. a. (2018, October 22). *The ai learner*. Retrieved from https://theailearner.com/2018/10/22/color-image/

Addcomposites. (2024). Retrieved from https://www.addcomposites.com/post/filament-winding

Python-based. (2025). Retrieved from https://github.com/python-based-Fiber-volume-fraction-calculation-in-microscopic-images

Canny, J. (1986). *A Computational Approach to Edge Detection*. Retrieved from https://ieeexplore.ieee.org/document/4767851

Shape-Detection. (2025). Retrieved from https://github.com/Sivamayura/Shape-Detection-with-Canny-and-Contours

Mikkelsen, L. P. (2021, April). Retrieved from https://www.sciencedirect.com/science/article/pii/S2352340921001529

Asfew, K. N. (2024). Retrieved from https://www.researchgate.net/publication/370055191_Investigation_of_fiber_content_evaluation_methods_of_carbon_fiber_reinforced_thermoplastic_composites, give me this as a reference